

Effects of continuous intravenous infusion with propofol on intestinal metabolites in rats

JIAYING LI¹, ZHONGJIE ZHANG¹, HONGYU LIU¹, XUTONG QU¹, XUEQING YIN¹,
LU CHEN¹, NANA GUO², CHANGSONG WANG² and ZHAODI ZHANG¹

Departments of ¹Anesthesiology and ²Critical Care Medicine, Harbin Medical University Cancer Hospital,
Harbin, Heilongjiang 150081, P.R. China

Received October 10, 2022; Accepted May 18, 2023

DOI: 10.3892/br.2023.1713

Abstract. Microbial metabolites play an important role in regulating intestinal homeostasis and immune responses. Propofol is a common anesthetic in clinic, but it is not clear whether it affects intestinal metabolites in rats. Tail vein puncture was performed after adaptive feeding for 1 month in eight 2-month-old rats and they were given continuous intravenous infusion of propofol for 3 h. The feces of rats were divided into different groups based on time periods, with before and after anesthesia with propofol on days 1, 3 and 7 labeled as groups P, A1, A3 and A7, respectively. The effect of continuous intravenous infusion with propofol on rat fecal metabolites was determined using the non-targeted metabolomics technique gas chromatography coupled with a time-of-flight mass spectrometer analysis. The types and contents of metabolites in rat feces were changed after continuous intravenous infusion with propofol, but the changes were not statistically significant. The contents of the metabolites 3-hydroxyphenylacetic acid and palmitic acid increased from day 3 to 7, and it was shown that the two metabolites were positively correlated at a statistically significant level. Linoleic acid decreased to its lowest level on day 3, and it returned to pre-anesthesia level on day 7. At the same time, linoleic acid metabolism was a metabolic pathway that was co-enriched 7 days after infusion with propofol. Spearman correlation analysis showed that there was significant correlation between some differential metabolites and differential microorganisms. It was observed that zymosterol 1, cytosin and elaidic acid were negatively correlated with *Alloprevotella* in the A3 vs. P group. In the A7 vs. P group, cortexolone 3 and coprostan-3-one were positively correlated with *Faecalibacterium*, whilst aconitic acid was negatively correlated with it. In conclusion, the present study revealed

statistically insignificant effects of continuous intravenous propofol on the intestinal metabolites in rats.

Introduction

Propofol, also known as 2,6-diisopropylphenol, is an intravenous, short-acting anesthetic that is widely used because it can induce and maintain general anesthesia, providing systematic sedation (1). Propofol has a fast onset of action of 10-50 sec and a short duration of action of 3-10 min, making anesthesia induction rapid and sensitive (2). Therefore, it is commonly used as a sedative in patients who are critically ill (2). Due to its pharmacokinetic properties, it can be infused continuously using an intravenous pump. In particular, it can be combined with opioids as part of a 'balanced anesthesia' program (3). It can also be used as a hypnotic in patients receiving mechanical ventilation and conscious sedation, especially during day surgery or non-invasive surgery, such as radiotherapy, endoscopy and MRI. This is because propofol carries reduced risks of nausea and vomiting compared with inhalation anesthetics, such as sevoflurane, in addition to the lack of air irritation (3,4). However, propofol is not without side effects, such as injection pain, apnea and low blood pressure. A serious adverse reaction is propofol-related infusion syndrome or propofol infusion syndrome, which is an umbrella term for a set of symptoms, including bradycardia, metabolic acidosis, hepatomegaly, rhabdomyolysis and/or myoglobinuria (5). Mortality can occur in extreme cases (5).

The possible relationship between adverse reactions after propofol infusion and microscopic changes in the body remain elusive. A number of studies have previously shown that some biologically active intestinal microbiota and microbial metabolites are closely associated with the homeostasis, etiology and prognosis of disease (6-8). Gut microbes rely on high-fiber food residues to maintain their normal structure and metabolism, with the production of the metabolite butyrate having a notable role in maintaining gut homeostasis and epithelial health (7). Butyrate can mediate the protective effect of dietary fiber against colorectal cancer through various mechanisms (7). Over the past decade, extensive attention has been paid in the study of the gut microbiome. In addition to 16S ribosomal RNA sequencing, metabolomic analysis is an effective method of understanding how the host and the microbiome communicate

Correspondence to: Professor Zhaodi Zhang, Department of Anesthesiology, Harbin Medical University Cancer Hospital, 150 Haping Road, Harbin, Heilongjiang 150081, P.R. China
E-mail: jody2021@yeah.net

Key words: anesthetic, propofol, metabolome, untargeted metabolomics, intravenous anesthesia, rats

in the gut environment (6). Microbial metabolites and products are becoming increasingly recognized as important signals regulating host physiology (8). In addition, they can serve as diagnostic markers of disease. Several studies have previously reported that short-chain fatty acid levels, including acetate, butyrate and propionate, are markedly reduced in patients with acute graft-vs.-host disease (aGVHD), which is in turn associated with increased GVHD severity and mortality (9). A recent study showed that continuous infusion with propofol exerts little effect on the intestinal flora (10). The present study was an extension of a previous study (10) to investigate the effect of propofol infusion on intestinal metabolites in rats.

In the current study, the feces of rats that received continuous intravenous infusions with propofol were collected before the intestinal signature of differential metabolites was analyzed at different time periods. Furthermore, a correlation analysis with existing intestinal flora results was carried out to assess the relationship between the flora and metabolite profiles.

Materials and methods

Ethics. The ethical approval reference number for the present study was KY2018-02 and was approved by the Regional Ethics Committee of the Cancer Hospital Affiliated to Harbin Medical University (Harbin, China) in December 2018.

Animals. A total of 16 2-month-old specific pathogen-free status, male Wistar International-Genetics-Standard rats (batch qualification no. 1100111911030133) provided by Beijing Weitong Lihua Experimental Animal Technology Co. Ltd. [license number: SCXK (Beijing, China) 2016-0006] were kept at room temperature $23\pm 1^{\circ}\text{C}$ and 20-30% humidity, with 12-h light/night cycle lighting with free movement. Food and water were available *ad libitum*. The feeding of animals was performed in accordance with the 'Guide for the care and use of laboratory animals'. The tail of every rat was labeled as T1-T16. Rats were adaptively housed for 1 month, after which the experiments were performed.

Criterion of loss of righting reflex (LORR) and recovery of righting reflex (RORR). In the present study, LORR was applied to reflect the suppression of consciousness in rats, whereas RORR was used to reflect the recovery of consciousness in rats. A rat was considered to have regained consciousness if it could voluntarily return to the prone position within 30 sec (11).

Deceased rats. Two unexplained rat deaths were confirmed upon feeding. Another six rats were excluded for experimental purposes because indwelling needles could not be inserted due to unsuccessful venipunctures. A total of eight rats with successful venipuncture were included in the present study, and these rats were thereafter re-numbered as R1-R8. The weight of every rat was measured before anesthesia (Table I). The average weight of the 8 rats was 384.0 ± 44.7 g.

Experimental design. Tail vein puncture was performed on every rat and an indwelling needle (no. 26) was inserted. After successful operation, a single dose (11 mg/kg) of propofol (Diprivan; X22027B; CordenPharma GmbH) was

administered for 1 min to every rat via tail-vein injection (i.v.) to induce LORR (12). After LORR, propofol was continuously injected into the rats tail vein for 3 h through an injection pump (SYS-52; Shenzhen Maiketian Biomedical Technology Co., Ltd.). The anesthetic maintenance dose was initially set at 40 mg/kg/h (12). The dose was adjusted based on changes in the body weight and respiratory rate of the rats. The respiratory rate was recorded every 5 min. The respiratory rate was kept in the range of 60-85 times/min. The RORR time of every rat is listed in Table I, where the average RORR time of the 8 rats was 30.1 ± 17.4 min. The rats were put back into the cage for further feeding after their righting reflex was completely recovered. Feces were collected from every rat before and on days 1, 3 and 7 after propofol infusion. The collection of feces was performed at 10 a.m. Feces were collected in sterile frozen tubes before being labeled and stored in a -80°C refrigerator. The feces of the rats were divided into different groups based on time periods, with before and after intervention on days 1, 3 and 7 labeled as groups P, A1, A3 and A7, respectively. Signs of severe distress in rats, such as apnea, behavioral limitations due to excessive pain and avoidance behaviors were considered the humane endpoints of the present study requiring immediate intervention. However, there were no cases requiring euthanasia due to observation of a humane endpoint and, therefore, animals were euthanized only at the end of the experimental period. After the completion of the current study, all experimental rats were euthanized. Every rat was given a caudal vein infusion with 6 mg of propofol, and then cervical dislocation was performed. Euthanasia was confirmed by loss of heartbeat and no response to foot pinch test.

Metabolite extraction and gas chromatography coupled with a time-of-flight mass spectrometer (GC-TOF-MS) analysis. In total, 50 ± 1 mg of fecal sample was transferred into a 2-ml tube, before 500 μl of pre-cold extraction mixture [methanol/chloroform (volume:volume)=3/1] with 10 μl internal standard (adonitol, 0.5 mg/ml stock) were added, mixed by vortex for 30 sec. The steel ball was then added, before the samples were processed with a 35-Hz grinding instrument for 4 min followed by ultrasonic treatment in an ice water bath for 5 min. This process was repeated three times. After centrifugation at 4°C for 15 min at $13,800 \times g$, 200 μl supernatant were transferred into a fresh 2-ml tube. To prepare the quality control (QC) sample, 50 μl of every sample were removed and mixed together. After evaporation in a vacuum concentrator, 30 μl of methoxyamination hydrochloride (20 mg/ml in pyridine) were added and incubated at 80°C for 30 min, before being derivatized by 40 μl N,O-Bis(trimethylsilyl)trifluoroacetamide reagent (1% Tri Methyl Chloro Silane, volume/volume) at 70°C for 1.5 h. Fecal samples from four different time points were used as pairwise control groups and GC-TOF-MS analysis was performed on them using an Agilent 7890 gas chromatograph (Agilent Technologies, Inc.), detailed by a previous study (13).

Data preprocessing and annotation. Raw data analysis, including peak extraction, baseline adjustment, deconvolution, alignment and integration, was performed using ChromaTOF® (version 4.3x; LECO Corporation) software. The LECO-Fiehn Rtx5 database (<https://fiehnlab.ucdavis.edu/projects/fiehnlib>) was used for metabolite identification by matching the mass

Table I. Weight and RORR time of every R (n=8).

Rat parameter	R1	R2	R3	R4	R5	R6	R7	R8	$\bar{x} \pm s$
Weight, in g	350.0	340.0	367.0	381.0	335.0	420.5	420.0	458.5	384.0±44.7
RORR time, in min	25.0	11.0	60.0	25.0	30.0	30.0	10.0	50.0	30.1±17.4

RORR, recovery of righting reflex; R, rat.

spectrum and retention index. Finally, the peaks detected in <50% of the QC samples or relative standard deviation >30% in the QC samples, were removed.

Metabolome and microbe association analysis. Pearson's correlation and Spearman's correlation analyses were used to determine whether there was a significant linear (Pearson's correlation) or monotonic (Spearman's correlation) relationship between the microbiome components or genes and a single metabolite of the metabolome. The redundancy analysis (RDA) or canonical correlation analysis (CCA) is a sorting method developed based on the corresponding analysis, combining the corresponding analysis with multiple regression analysis to perform multiple linear regressions of two sets of data for every calculation during the iteration of the corresponding analysis. The RDA is based on a linear model, whereas the CCA is based on a unimodal model. Decision Curve Analysis was performed with the species-sample data to deduce the size of the first axis of lengths of gradient in the analysis results. If >4.0, then CCA would be preferred. If 3.0-4.0, both RDA and CCA were used. However, if <3.0, then RDA was preferred. Differential genes and differential metabolites were simultaneously mapped to the Kyoto Encyclopedia of Genes and Genomes (KEGG; <http://www.kegg.jp/kegg/pathway.html>) pathway database through the 'Pathview' package of R (v1.26.0; <https://pathview.uncc.edu/>) to obtain their common pathway information. Nodes enriched for the differential compounds and differential genes in the significant metabolic pathways were then shown in different colors, representing differential compounds and genes in metabolic pathways.

Statistical analysis. In the present study SPSS (v21.0; IBM Corp.) was used for statistical analysis. SIMCA® software (v16.0.2; Sartorius Stedim Data Analytics AB) was used to model and analyze data, including principal component analysis (PCA) and orthogonal projections to latent structures-discriminant analysis (OPLS-DA). Differential metabolites were screened using the paired Student's t-test and the variable importance in the projection (VIP) of the first principal component of OPLS-DA model ($P < 0.05$ and $VIP > 1$ were considered to indicate a statistically significant difference). The quantitative values of differential metabolites were calculated using the Euclidean distance matrix, and the differential metabolites were clustered using complete linkage method. Finally, the heatmap of differential metabolites following hierarchical clustering analysis was shown. Key pathways with the highest correlation with the metabolite differences were found by metabolic pathway enrichment

analysis. Spearman correlation analysis was used to assess the correlation between the microorganisms and metabolites.

Results

Changes in the types and contents of metabolites. In the score scatterplot from the PCA model, the distribution of the four sample groups was found to be relatively concentrated on a whole (Fig. 1A). Comparisons between the A1 and P groups (Fig. 1B), A1 and A3 groups (Fig. 1C), P and A3 groups (Fig. 1D), P and A7 groups (Fig. 1F) and between the A7 and A1 groups (Fig. 1G), showed a relatively centralized trend. Only the A7 and A3 group comparison revealed some degree of separation (Fig. 1E). These results suggested that continuous intravenous infusion with propofol exerted little effect on the type and content of metabolites in the fecal samples.

Differential metabolites. To deduce the actual difference among the groups and screen for effective differential metabolites, OPLS-DA was used to analyze the results. The results of OPLS-DA analysis showed that the samples between A1 and P (Fig. 2A), A3 and P (Fig. 2C), A7 and P (Fig. 2E), A3 and A1 (Fig. 2G), A7 and A1 (Fig. 2I) and between A7 and A3 (Fig. 2K) were all separated. This suggested that there were differential metabolites among the groups. Bringing the samples further into the permutation tests within OPLS-DA, comparisons between the models of A1 and P (Fig. 2B), A3 and P (Fig. 2D), A7 and P (Fig. 2F), A3 and A1 (Fig. 2H) and between A7 and A3 (Fig. 2L), yielded robustness and no over-fitting phenomenon. Only comparison between A7 and A1 did not yield robustness (Fig. 2J). This finding suggested that there was no significant difference in intestinal metabolites between days 1 and 7 after intravenous propofol anesthesia. Metabolites with $VIP > 1$ and $P < 0.05$ were considered to be differential metabolites. Table II listed the differential metabolites' P-value and VIP. As it can be seen in Table II, from day 3 to 7 the content of 3-hydroxyphenylacetic and palmitic acid increased significantly. The heatmap of differential metabolites following hierarchical clustering analysis is shown in Fig. 3. It was revealed that a number of differential metabolites showed continuous changes. In particular, the levels of cytosin and aconitic acid were consistently and significantly decreased throughout the 7 days after anesthesia (Fig. 3A-C). In addition, the levels of linoleic acid methyl ester and zymosterol 1 decreased throughout the 3 days after anesthesia, but they returned to pre-anesthetic levels on day 7 (Fig. 3A, B and F). The levels of linoleic acid dropped to a minimum on day 3, but they recovered on day 7 (Fig. 3B and F). By contrast, pipercolinic acid and guanidine levels were both significantly

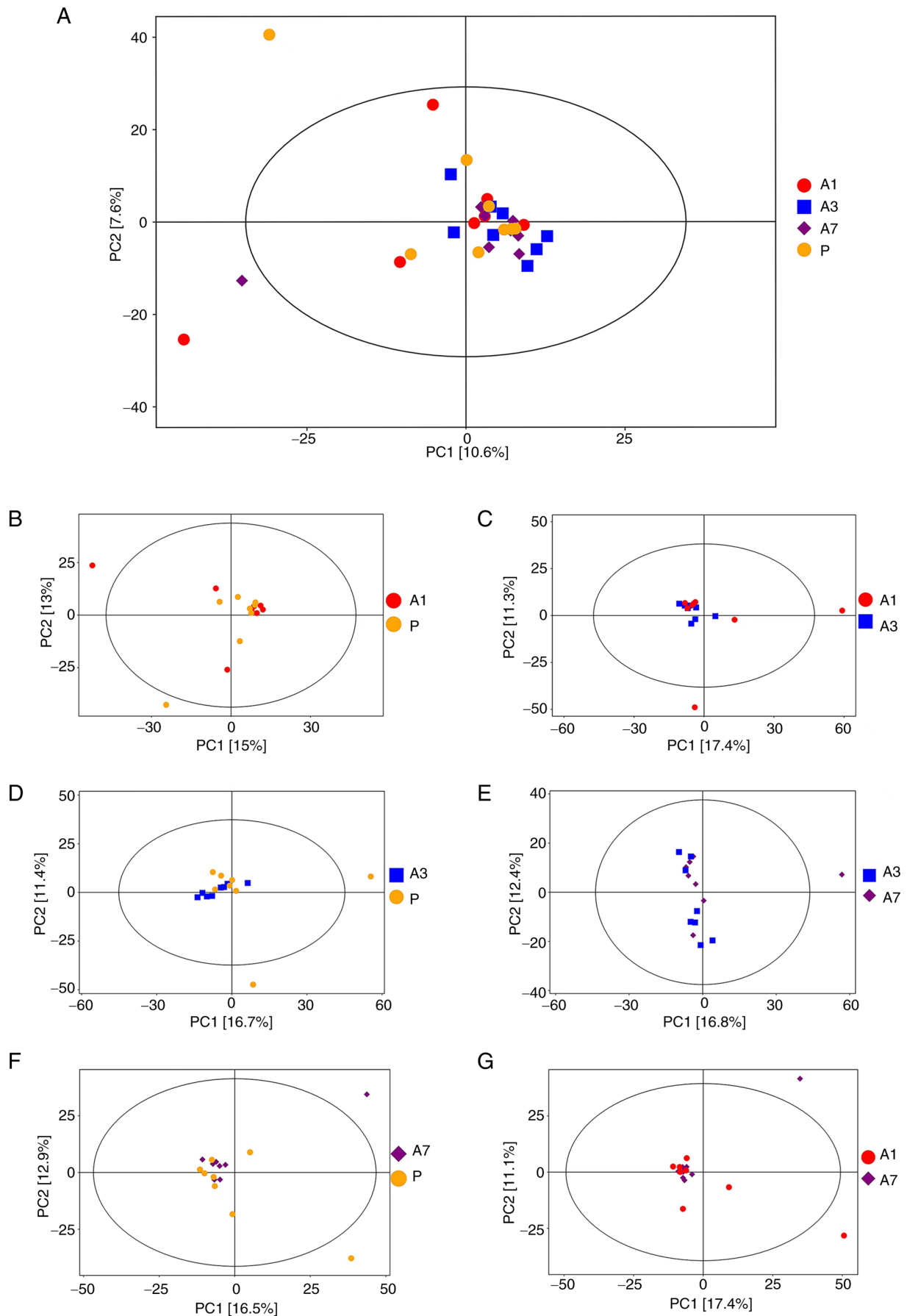


Figure 1. Score scatter plot of PCA model. (A) Score scatter plot for PCA model TOTAL, (B) group P vs. A1, (C) group A1 vs. A3, (D) group P vs. A3, (E) group A3 vs. A7, (F) group P vs. A7 and (G) group A1 vs. A7. Every scatter point represents a sample. The closer the distribution of sample points is, the more similar the type and content of metabolites in the samples are. $n=8$ per group. The samples were all within 95% confidence intervals. PCA, principal component analysis; P, before intervention; A3, after intervention on day 3; after intervention on 7.

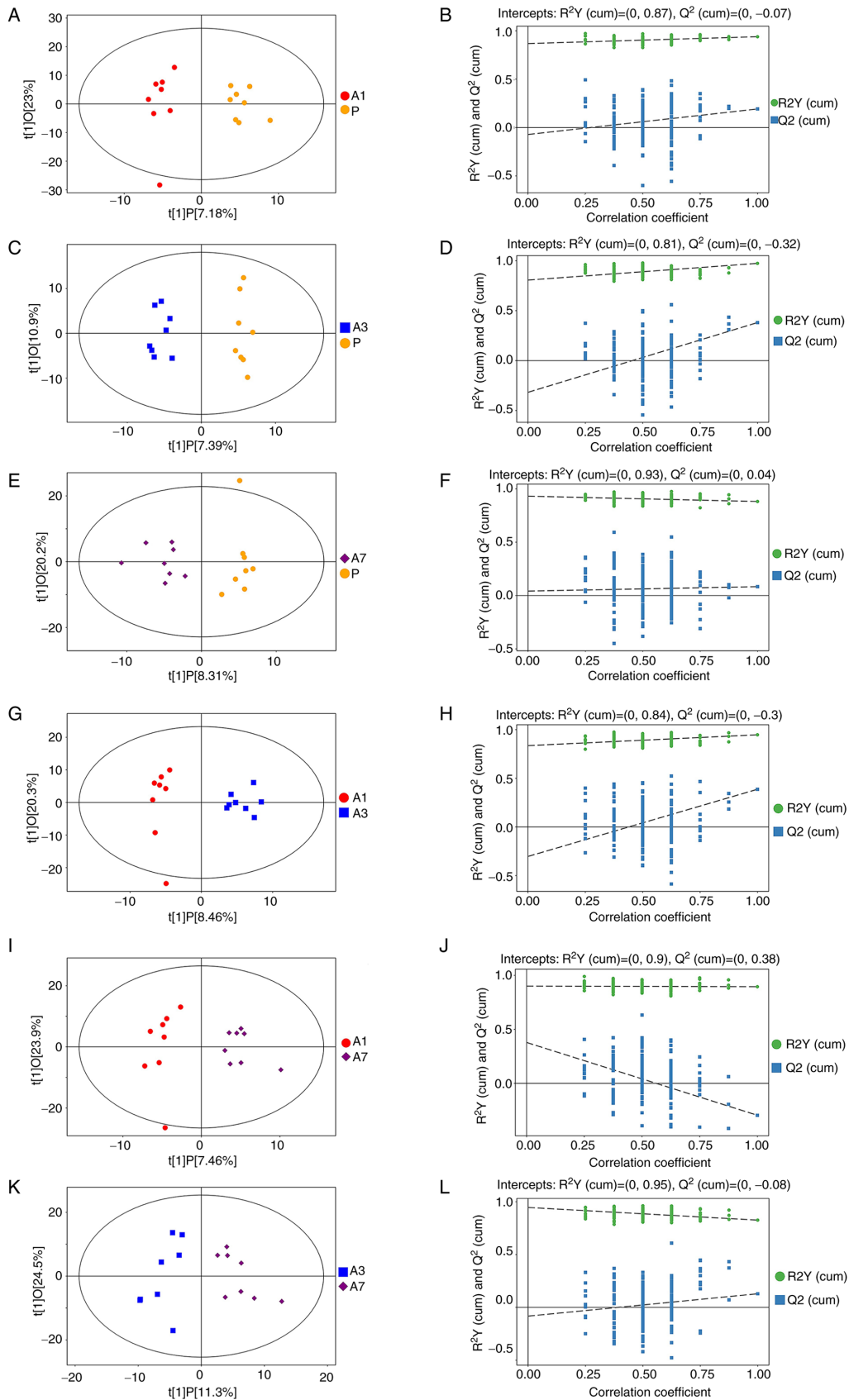


Figure 2. Score scatter plot and permutation test of OPLS-DA model. (A and B) Group P vs. A1, (C and D) group P vs. A3, (E and F) group P vs. A7, (G and H) group A1 vs. A3, (I and J) group A1 vs. A7 and (K and L) group A3 vs. A7. In the score scatter plot of OPLS-DA model, horizontal coordinate $t[1]P$ represents the predicted principal component score of the first principal component, showing the differences between sample groups; vertical coordinate $t[1]O$ represents the orthogonal principal component score, showing the differences within the sample group. Every scatter represents a sample, and the shape and color of the scatter represent different experimental groups. The farther the transverse distance between samples, the greater the differences between groups. The closer the longitudinal distance, the more improved the repeatability was within the group. $n=8$ per group, the samples were all within 95% confidence intervals. Permutation test of OPLS-DA model verified the robustness of the OPLS-DA model. OPLS-DA, orthogonal projections to latent structures-discriminant analysis; P, before intervention; A3, after intervention on day 3; after intervention on 7.

Table II. Statistics of differential metabolite outcomes between groups.

Group	Peak	VIP	P-VALUE	Q-VALUE	FOLD CHANGE	LOG_ FOLDCHANGE	Variation tendency
P-A1	Linoleic acid methyl ester	1.3551	0.0103	1	0.4355	-1.1994	Down
P-A1	Zymosterol 1	1.6643	0.0162	1	0.4971	-1.0085	Down
P-A1	Cytosin	1.4682	0.0383	1	0.5220	-0.9379	Down
P-A1	Pipecolic acid	1.2355	0.0424	1	3.3086	1.7262	Up
P-A1	Aconitic Acid	1.1256	0.0313	1	0.6182	-0.6938	Down
P-A1	Guanosine	2.3050	0.0438	1	1.9521	0.9650	Up
P-A3	Linoleic acid	2.8319	0.0014	0.2425	0.6045	-0.7262	Down
P-A3	Elaidic acid	2.7986	0.0017	0.2635	0.6515	-0.6181	Down
P-A3	Linoleic acid methyl ester	2.3945	0.0217	0.7570	0.5256	-0.9279	Down
P-A3	Zymosterol 1	2.4409	0.0000	0.0080	0.1252	-2.9976	Down
P-A3	Cytosin	2.4346	0.0055	0.4427	0.4020	-1.3149	Down
P-A3	Galactinol 3	1.6365	0.0273	0.7969	0.3273	-1.6113	Down
P-A3	Aconitic Acid	1.9367	0.0026	0.2942	0.3882	-1.3650	Down
P-A7	Cytosin	1.0576	0.0115	1	0.4319	-1.2113	Down
P-A7	Coprostan-3-one	1.2726	0.0112	1	1.8257	0.8685	Up
P-A7	Cortexolone 3	1.7122	0.0351	1	1.5252	0.6090	Up
P-A7	Naringenin 2	1.2024	0.0426	1	1.7064	0.7709	Up
P-A7	Aconitic Acid	1.6468	0.0221	1	0.5612	-0.8333	Down
P-A7	2-Hydroxyquinoline	2.3604	0.0343	1	0.5065	-0.9813	Down
A1-A3	Zymosterol 1	1.7887	0.0373	1	0.2519	-1.9891	Down
A1-A3	Pipecolic acid	1.9042	0.0332	1	0.2546	-1.9736	Down
A1-A3	Guanosine	1.3697	0.0183	1	0.3933	-1.3462	Down
A1-A3	2-Hydroxyquinoline	1.4066	0.0285	1	0.5283	-0.9206	Down
A3-A7	Linoleic acid	2.1390	0.0418	0.6866	1.6807	0.7491	Up
A3-A7	Palmitic acid	1.7825	0.0275	0.6866	1.3943	0.4796	Up
A3-A7	3-hydroxyphenylacetic acid	1.7011	0.0253	0.6866	1.3354	0.4172	Up
A3-A7	3-Hydroxypyridine	1.6606	0.0285	0.6866	1.2469	0.3183	Up
A3-A7	Zymosterol 1	1.2452	0.0398	0.6866	4.7028	2.2335	Up
A3-A7	L-Threose 1	1.6325	0.0286	0.6866	1.2289	0.2974	Up
A1-A7	Pipecolic acid	1.2104	0.0423	1	0.2981	-1.7462	Down
A1-A7	L-Threose 1	2.0590	0.0366	1	1.2338	0.3031	Up
A1-A7	2-Hydroxyquinoline	2.1475	0.0138	1	0.4385	-1.1894	Down

P, A1, A3, A7 represent before and after intervention on days 1, 3 and 7, respectively; VIP, variable importance in the projection.

elevated on day 1, and then gradually recovered on day 3 (Fig. 3A and D).

Metabolic pathways. The differential metabolites in the present study were then incorporated into KEGG and PubChem database (<https://pubchem.ncbi.nlm.nih.gov/>) for metabolic pathway analysis, the results of which are shown in the bubble map in Fig. 4. 'Linoleic acid metabolism' was found to be a commonly enriched metabolic pathway in the A3 vs. P and A7 vs. A3 groups (Fig. 4A and B).

Metabolome and microbe association analysis. A previous study showed that continuous intravenous infusion with propofol ~3 h resulted in changes in the gut microbe profile (10). Spearman correlation analysis was therefore performed to explore whether there was a correlation between

different species of microorganisms and various metabolites among the aforementioned groups (Fig. 5). It was observed that zymosterol 1, cytosin and elaidic acid were negatively correlated with *Alloprevotella* in the A3 vs. P group (Fig. 5A). In the A7 vs. P group, cortexolone 3 and coprostan-3-one were positively correlated with *Faecalibacterium*, whilst aconitic acid was negatively correlated with it (Fig. 5B). In addition, *Alloprevotella* and *Faecalibacterium* were the different species of microbes found in the previous studies (10).

Discussion

The present study was the first to investigate the effects of continuous intravenous administration of propofol on fecal metabolites in rats using an untargeted metabolomics technique. PCA and OPLS-DA analyses showed that although

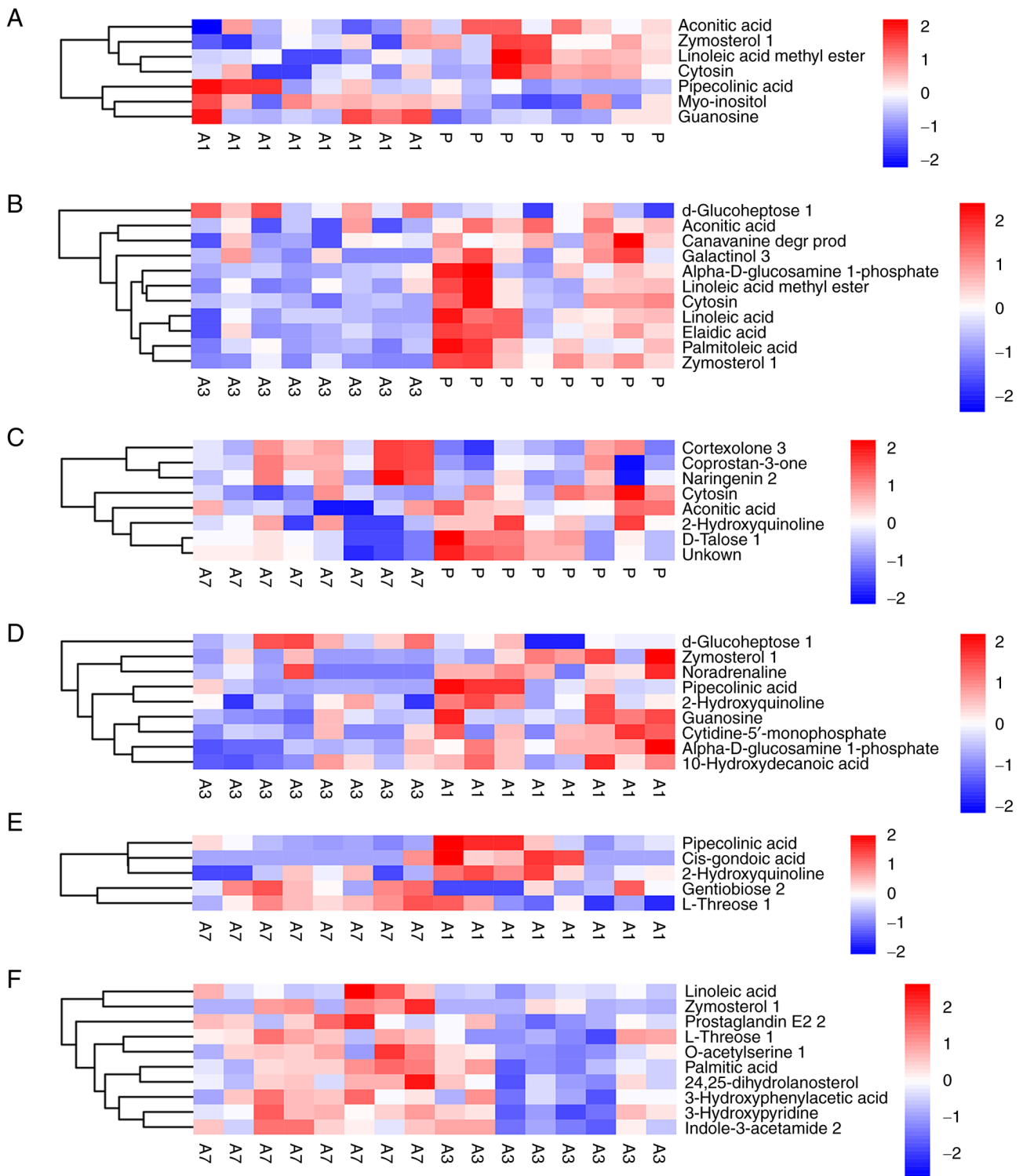


Figure 3. Heatmap of hierarchical clustering analysis. (A) Group P vs. A1, (B) group P vs. A3, (C) group P vs. A7, (D) group A1 vs. A3, (E) group A1 vs. A7, (F) group A3 vs. A7. The abscissa represents different experimental groups, the ordinate represents the different metabolites compared in the group, and the color blocks at different positions represent the relative expression levels of metabolites at corresponding positions. Red indicates that the substance is highly expressed in the group, and blue indicates that the substance is low expressed in the group. n=8 per group. The figures show the changes of quantitative values of differential metabolites in different groups. P, before intervention; A3, after intervention on day 3; after intervention on 7.

the types and levels of excreta metabolites in rats changed on days 1, 3 and 7 after the continuous intravenous infusion with propofol, the changes were not statistically significant. A similar previous study found that continuous intravenous infusion with propofol has little effect on the intestinal flora of male Wistar rats (10). The present study served as an

extension of this previous study (10), which further revealed the effects of continuous intravenous infusion with propofol on the intestinal microenvironment of rats from the perspective of metabolomics.

Propofol is a potent intravenous hypnotic drug and is typically formulated as an Intralipid®-based emulsion (Fresenius

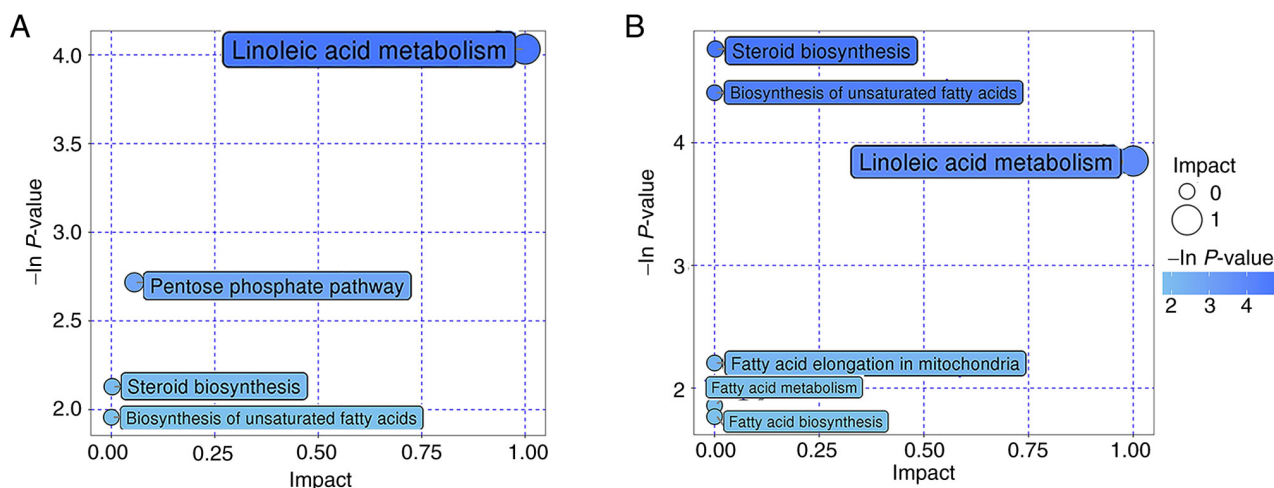


Figure 4. Bubble diagram of metabolic pathways. Groups (A) A3 vs. P and (B) groups A7 vs. A3. In the bubble diagram, every bubble represents a metabolic pathway. The abscissa and bubble size represent the impact factor of the path in topology analysis. The larger the bubble size is, the greater the impact factor is. The vertical coordinate of the bubble and bubble color represent the P-value of enrichment analysis. P, before intervention; A3, after intervention on day 3; after intervention on 7.

Kabi Ltd.) containing the same ingredients, namely soybean oil (100 mg/ml), glycerol (22.5 mg/ml) and egg lecithin (12 mg/ml) (14). Due to the infusion with this lipid formulation, propofol can cause adverse effects, such as metabolic acidosis, rhabdomyolysis, hyperlipidemia and enlarged fatty liver (15). The liver is the main site of propofol metabolism, but the small intestine also participates in this process (14). A study has previously indicated that compared with inhalation anesthesia, propofol anesthesia is associated with lower incidence of early postoperative cognitive dysfunction (POCD) in elderly patients (16). Another study on the effects of anesthetics on the human serum metabolome showed that after the continuous infusion with propofol for 1 h (1.7 $\mu\text{g/ml}$; $n=40$), 37 metabolites demonstrate notable changes in all intergroup comparisons. These were found in the metabolite subgroups of lipoprotein, fatty acid, glycerides and phospholipids (17). However, the effect of continuous infusion with propofol on fecal metabolites remains elusive.

The present study showed that there were various differential metabolites in the stool samples of rats collected at different time periods after anesthesia, with comparisons carried out between the pre- and post-treatment time periods. From day 3 to 7 after the continuous intravenous infusion with propofol, the content of 3-hydroxyphenylacetic and palmitic acid increased significantly. The metabolite 3-hydroxyphenylacetic acid belongs to the aromatic family. A previous study has shown that 3-hydroxyphenylacetic acid is notably elevated in the urine of children with autism, and it is positively correlated with the *Clostridium* species of bacteria (18). In a previous study, *Clostridium* was revealed to be a differential microbe (10), before and after the continuous intravenous infusion with propofol, which has also coincidentally been found to be markedly enriched in the feces of patients with autism (19). Palmitic acid is the most abundant saturated fatty acid in the human body; it can either be provided through diet, or synthesized endogenously from other fatty acids, carbohydrates and amino acids (20). In the intestines, palmitic acid has been shown to be able to modulate the immune system

by inducing monocyte activation and stimulating proinflammatory responses in human immune cells (21,22). Disruption of the palmitic acid homeostatic balance has been previously implicated in a range of pathophysiological conditions, such as atherosclerosis, neurodegenerative diseases and cancer, mainly due to aberrant endogenous palmitic acid biosynthesis (20). Palmitic acid in urine has been previously reported to serve as a potential biomarker for post-stroke depression (23).

A number of other differential metabolites also showed dynamic changes after propofol anesthesia, such that Spearman correlation analysis revealed significant correlation between some differential metabolites and differential microorganisms. Pipecolinic acid was significantly increased on day 1 after anesthesia, but returned to pre-anesthesia levels on day 3. A serum metabolomics study in patients with new-onset type 2 diabetes (T2D) revealed that pipecolinic acid can serve as a biomarker for T2D prediction, with a notable association between pipecolinic acid and cholinergic receptor muscarinic 3 (rs535514) (24). Pipecolinic acid has not been well studied as an intestinal metabolite, with the relationship to its host therefore being poorly understood. Ou *et al* (25) previously revealed that pipecolinic acid levels in the fecal metabolites have a notable positive correlation with defecation frequency in patients with constipation. In addition, the alleviation of constipation has been found to be induced by *Lactobacillus casei*, a Shirota strain (25). The present study demonstrated that pipecolinic acid was significantly negatively correlated with *Alloprevotella* but positively correlated with *Blautia* in groups A1-A3. This suggested that continuous infusion with propofol may cause the fluctuation of pipecolinic acid content by altering the physiology of *Alloprevotella* and *Blautia*. However, further verification is required.

In the present study, the levels of cytosin and aconitic acid continued to decrease significantly within 7 days after propofol infusion. These are rare metabolites that showed a one-way fluctuation, among the differential metabolites that were found. Since information on cytosin remains insufficient, whether cytosin serves an important mechanism of action in

living organisms remains unknown. By contrast, aconitic acid, also known as propene-1,2,3-tricarboxylic acid, is an unsaturated tricarboxylic acid used in the chemical industry as raw material for the organic synthesis of other compounds, such as flavoring agents (26). Aconitic acid can also serve a variety of biological roles in cells; serving as an intermediate in the tricarboxylic acid cycle and providing certain plants unique survival advantages as an antifeedant and antifungal agent, and a means of storing fixed carbon pools (27). In a study on urine metabolomics, Kwan *et al* (28) previously revealed that 13 metabolites, including aconitic acid, are associated with diabetic kidney disease. In addition, in a further prospective cohort study (28), 3-hydroxyisobutyrate and aconitic acid levels were found to be associated with higher and lower risk of kidney failure with replacement therapy, that is initiation of dialysis or receipt of transplant, respectively. Another untargeted metabolomics study of serum (29) found that 11 metabolites, including aconitic acid, were the optimal markers for the diagnosis of intracerebral hemorrhage. In addition, concerning the metagenomics and metabolomic integration analysis of biofecal matter, a controlled trial in patients with arteriosclerosis and normal control individuals (30), showed a high abundance and centrality of *Flavonifractor plautii* in normal control individuals and the absence of this species in the microbiome of patients with arteriosclerosis. Furthermore, increased cis-acetic acid has been found to be the main effector of the protective effect of *Flavonifractor plautii* against arteriosclerosis. Cis-acetic acid is the isomer of aconitic acid (30). These observations suggest that aconitic acid likely serves an important role as a marker in different biological materials. The levels of aconitic acid continued to decrease in the present study. However, whether this specific metabolite can be used as a potential biomarker for the occurrence of propofol-related complications or for the mechanism of action of propofol anesthesia on the human body remains a topic of further research.

Linoleic acid is not only the most abundant polyunsaturated fatty acid (PUFA) in human nutrition, but also an important component of the cellular membrane structure (31). Linoleic acid is the direct precursor of a wide range of other bioactive ω 6 PUFAs, such that the metabolites of linoleic acid, represented by arachidonic acid, can promote a potent proinflammatory response in rats (32,33). In the gut, the dynamic balance of linoleic acid is maintained by both dietary intake and bacterial metabolism (34). Linoleic acid can be metabolized to 10-hydroxy-cis-12-octadecenoic acid by the gut microbiota, which can prevent epithelial barrier impairment in Caco-2 cells and ameliorate intestinal inflammation by suppressing TNF receptor 2 upregulation (34). A previous study found that novel propofol-AA esters exhibit unique anticancer activity and can inhibit tumor growth (35). The present study found that linoleic acid metabolism was the metabolic pathway that was particularly enriched in both the P vs. A3 and A3 vs. A7 groups, suggesting that propofol is likely to cause continuous changes in fecal linoleic acid levels by affecting the linoleic acid metabolism pathway.

Another study revealed that the most notable changes in the intestinal flora of mice are observed on day 7 after the continuous inhalation of sevoflurane for 4 h, accompanied by changes in metabolites associated with different

microorganisms (36). However, this previous study (36) and the present study revealed that after the continuous intravenous administration of propofol, there are no significant changes in the intestinal flora or intestinal metabolites of mice (10). The effects of pathological changes during disease conditions after general anesthesia on changes in the intestinal microecological environment caused by these two anesthetics remain outstanding issues that require future clarification. For example, the incidence of POCD after propofol anesthesia is lower compared with that after sevoflurane anesthesia (16), but the potential role of the intestinal microecosystem in this remains unknown.

The present study is associated with a number of limitations. Propofol is widely used in patients of all ages. However, in the present study, 2-month-old adult male rats were used, meaning that the study is lacking in experimental data from juvenile, elderly and female rats. The effects of age and sex on the effects of propofol anesthesia will need verification in future studies. Another limitation refers to the potential effects of hypoxia and respiratory depression on intestinal microbes and metabolites. Intubation and oxygen delivery were not performed in the present study. Although the respiratory rate of rats was closely observed, this possibility cannot be completely ruled out. In addition to hypoxia, anesthesia may cause changes in physiological indicators, such as hypothermia, hypercapnia and hypotension in rats. Tripathi *et al* (37) previously simulated sleep apnea syndrome by exposing mice to intermittent hyperoxia and hypercapnia for 6 weeks. The authors found that this intervention can lead to changes in the intestinal microbiome and metabolites in mice (37). Few studies have investigated these contents, where the described interventions of mice that exhibited positive results are long term, ranging from 30 days to 6 weeks. The short 3-h term effects of hypoxia, hypothermia and hypercapnia on the intestinal microbiome and metabolites have not been verified. In addition, as continuous database improvements, the utility of measurement instruments is also constantly improving. Only 6,810 metabolites were identified in the feces of the human metabolome database. This may be an order of magnitude lower compared with the true chemical diversity of the metabolites in the human gastrointestinal flora (38). Resolution of these issues relies on the development and improvement of metabolomics software tools related to metabolite identification and diverse data types. In the present study, only GC-TOF-MS was performed based on a metabolomic analysis, and it was shown that continuous intravenous infusion with propofol had little effect on rat intestinal metabolites. The mechanism by which propofol can regulate gut microbiota metabolites will need to be investigated. In addition, attempts can be made to explain the underlying mechanism of the side effects or adverse post-operative consequences following propofol application from the perspective of intestinal microbiota metabolites for prevention purposes.

In conclusion, the present study revealed statistically insignificant effects of continuous intravenous propofol on the intestinal metabolites in rats. However, additional studies are required to confirm this, in particular in human samples.

Acknowledgements

Not applicable.

Funding

This work was supported by the Outstanding Youth Project Foundation of Harbin Medical University Cancer Hospital (grant no. JCQN2021-05), the Haiyan Research Foundation (grant no. JJZD2022-04), and the Natural Science Foundation of Heilongjiang Province (grant nos. YQ2020H038 and JJ2020YX0472).

Availability of data and materials

The datasets used and/or analyzed during the current study are available from the corresponding author on reasonable request.

Authors' contributions

JL and ZhZ conceived the study, designed experiments, analyzed and interpreted data, and wrote the manuscript. HL, XQ, XY, NG and LC interpreted data. ZhaZ and CW designed experiments, confirmed the authenticity of all the raw data and gave final approval of the manuscript to be published. All authors have read and approved the final manuscript.

Ethics approval and consent to participate

The ethical approval reference number for the study was KY2018-02 and was approved by the Regional Ethics Committee of the Cancer Hospital Affiliated to Harbin Medical University in December 2018.

Patient consent for publication

Not applicable.

Competing interests

The authors declare that they have no competing interests.

References

- Budic I, Jevtovic Stojmenov T, Pavlovic D, Marjanovic V, Djordjevic I, Stevic M and Simic D: Clinical importance of potential genetic determinants affecting propofol pharmacokinetics and pharmacodynamics. *Front Med (Lausanne)* 9: 809393, 2022.
- Koriyama H, Duff JP, Guerra GG and Chan AW; Sedation Withdrawal and Analgesia Team: Is propofol a friend or a foe of the pediatric intensivist? Description of propofol use in a PICU*. *Pediatr Crit Care Med* 15: e66-e71, 2014.
- Dinis-Oliveira RJ: Metabolic profiles of propofol and fospropofol: Clinical and forensic interpretative aspects. *Biomed Res Int* 2018: 6852857, 2018.
- Asghar MU, Cheema HA, Tanveer K and Leinwand J: Propofol infusion and acute pancreatitis: A review. *Am J Ther* 27: e371-e374, 2020.
- Walsh CT: Propofol: Milk of Amnesia. *Cell* 175: 10-13, 2018.
- Sanada S, Suzuki T, Nagata A, Hashidume T, Yoshikawa Y and Miyoshi N: Intestinal microbial metabolite stercobilin involvement in the chronic inflammation of ob/ob mice. *Sci Rep* 10: 6479, 2020.
- Wu X, Wu Y, He L, Wu L, Wang X and Liu Z: Effects of the intestinal microbial metabolite butyrate on the development of colorectal cancer. *J Cancer* 9: 2510-2517, 2018.
- Xing PY, Pettersson S and Kundu P: Microbial metabolites and intestinal stem cells tune intestinal homeostasis. *Proteomics* 20: e1800419, 2020.
- Lin D, Hu B, Li P, Zhao Y, Xu Y and Wu D: Roles of the intestinal microbiota and microbial metabolites in acute GVHD. *Exp Hematol Oncol* 10: 49, 2021.
- Guo N, Zhang Z, Han C, Chen L, Zheng X, Yu K, Zhang Z and Wang C: Effects of continuous intravenous infusion with propofol on intestinal flora in rats. *Biomed Pharmacother* 134: 111080, 2021.
- Shirasaka T, Yonaha T, Onizuka S and Tsuneyoshi I: Effects of orexin-A on propofol anesthesia in rats. *J Anesth* 25: 65-71, 2011.
- Wang Y, Yu T, Yuan C, Yuan J, Luo Z, Pan Y, Zhang Y, Zhang Y and Yu B: Effects of propofol on the dopamine, metabolites and GABAA receptors in media prefrontal cortex in freely moving rats. *Am J Transl Res* 8: 2301-2308, 2016.
- Liu H, Yin X, Li J, Cao Y, Wang Y, Yin W, Zhuo Z, Chen L, Zhang Z, Qu X, *et al*: Preoperative intestinal microbiome and metabolome in elderly patients with delayed neurocognitive recovery. *Anaesth Crit Care Pain Med* 41: 101140, 2022.
- Sahinovic MM, Struys MMRF and Absalom AR: Clinical pharmacokinetics and pharmacodynamics of propofol. *Clin Pharmacokinet* 57: 1539-1558, 2018.
- Kam PC and Cardone D: Propofol infusion syndrome. *Anaesthesia* 62: 690-701, 2007.
- Xu D, Yang W and Zhao G: Effect of propofol and inhalation anesthesia on postoperative cognitive dysfunction in the elderly: A meta-analysis. *Nan Fang Yi Ke Da Xue Xue Bao* 32: 1623-1627, 2012 (In Chinese).
- Nummela AJ, Laaksonen LT, Laitio TT, Kallionpaa RE, Langsjö JW, Scheinin JM, Vahlberg TJ, Koskela HT, Aittomäki V, Valli KJ, *et al*: Effects of dexmedetomidine, propofol, sevoflurane and S-ketamine on the human metabolome: A randomised trial using nuclear magnetic resonance spectroscopy. *Eur J Anaesthesiol* 39: 521-532, 2022.
- Xiong X, Liu D, Wang Y, Zeng T and Peng Y: Urinary 3-(3-Hydroxyphenyl)-3-hydroxypropionic Acid, 3-Hydroxyphenylacetic Acid, and 3-Hydroxyhippuric acid are elevated in children with autism spectrum disorders. *Biomed Res Int* 2016: 9485412, 2016.
- Finegold SM, Molitoris D, Song Y, Liu C, Vaisanen ML, Bolte E, McTeague M, Sandler R, Wexler H, Marlowe EM, *et al*: Gastrointestinal microflora studies in late-onset autism. *Clin Infect Dis* 35 (Suppl 1): S6-S16, 2002.
- Carta G, Murru E, Banni S and Manca C: Palmitic Acid: Physiological role, metabolism and nutritional implications. *Front Physiol* 8: 902, 2017.
- Nicholas DA, Zhang K, Hung C, Glasgow S, Aruni AW, Unternaehrer J, Payne KJ, Langridge WHR and De Leon M: Palmitic acid is a toll-like receptor 4 ligand that induces human dendritic cell secretion of IL-1 β . *PLoS One* 12: e0176793, 2017.
- Tran TT, Postal BG, Demignot S, Ribeiro A, Osinski C, Pais de Barros JP, Blachnio-Zabielska A, Leturque A, Rousset M, Ferre P, *et al*: Short term palmitate supply impairs intestinal insulin signaling via ceramide production. *J Biol Chem* 291: 16328-16338, 2016.
- Chen J, Lv YN, Li XB, Xiong JJ, Liang HT, Xie L, Wan CY, Chen YQ, Wang HS, Liu P and Zheng HQ: Urinary metabolite signatures for predicting elderly stroke survivors with depression. *Neuropsychiatr Dis Treat* 17: 925-933, 2021.
- Ouyang Y, Qiu G, Zhao X, Su B, Feng D, Lv W, Xuan Q, Wang L, Yu D, Wang Q, *et al*: Metabolome-Genome-Wide association study (mGWAS) reveals novel metabolites associated with future type 2 diabetes risk and susceptibility loci in a case-control study in a Chinese prospective cohort. *Glob Chall* 5: 2000088, 2021.
- Ou Y, Chen S, Ren F, Zhang M, Ge S, Guo H, Zhang H and Zhao L: *Lactobacillus casei* strain shirota alleviates constipation in adults by increasing the pipercolinic acid level in the Gut. *Front Microbiol* 10: 324, 2019.
- Takiguchi A, Yoshioka I, Oda Y, Ishii Y and Kirimura K: Constitutive production of aconitate isomerase by *Pseudomonas* sp. WU-0701 in relation to trans-acetic acid assimilation. *J Biosci Bioeng* 131: 47-52, 2021.
- Bruni GO and Klasson KT: Aconitic acid recovery from renewable feedstock and review of chemical and biological applications. *Foods* 11: 573, 2022.
- Kwan B, Fuhrer T, Zhang J, Darshi M, Van Espen B, Montemayor D, de Boer IH, Dobre M, Hsu CY, Kelly TN, *et al*: Metabolomic markers of kidney function decline in patients with diabetes: Evidence from the chronic renal insufficiency cohort (CRIC) study. *Am J Kidney Dis* 76: 511-520, 2020.

29. Chen L, Wang S, Zhang Y, Li Y, Zhang X, Ma J, Zou X, Yao T, Li S, Chen J, *et al*: Multi-omics reveals specific host metabolism-microbiome associations in intracerebral hemorrhage. *Front Cell Infect Microbiol* 12: 999627, 2022.
30. Luo S, Zhao Y, Zhu S, Liu L, Cheng K, Ye B, Han Y, Fan J and Xia M: Flavonifractor plautii protects against elevated arterial stiffness. *Circ Res* 132: 167-181, 2023.
31. Whelan J and Fritsche K: Linoleic acid. *Adv Nutr* 4: 311-312, 2013.
32. Choque B, Catheline D, Rioux V and Legrand P: Linoleic acid: Between doubts and certainties. *Biochimie* 96: 14-21, 2014.
33. Fritsche KL: Too much linoleic acid promotes inflammation-doesn't it? *Prostaglandins Leukot Essent Fatty Acids* 79: 173-175, 2008.
34. Miyamoto J, Mizukure T, Park SB, Kishino S, Kimura I, Hirano K, Bergamo P, Rossi M, Suzuki T, Arita M, *et al*: A gut microbial metabolite of linoleic acid, 10-hydroxy-cis-12-octadecenoic acid, ameliorates intestinal epithelial barrier impairment partially via GPR40-MEK-ERK pathway. *J Biol Chem* 290: 2902-2918, 2015.
35. Khan AA, Alam M, Tufail S, Mustafa J and Owais M: Synthesis and characterization of novel PUFA esters exhibiting potential anticancer activities: An in vitro study. *Eur J Med Chem* 46: 4878-4886, 2011.
36. Han C, Zhang Z, Guo N, Li X, Yang M, Peng Y, Ma X, Yu K and Wang C: Effects of sevoflurane inhalation anesthesia on the intestinal microbiome in mice. *Front Cell Infect Microbiol* 11: 633527, 2021.
37. Tripathi A, Melnik AV, Xue J, Poulsen O, Meehan MJ, Humphrey G, Jiang L, Ackermann G, McDonald D, Zhou D, *et al*: Intermittent hypoxia and hypercapnia, a hallmark of obstructive sleep apnea, alters the gut microbiome and metabolome. *mSystems* 3: e00020-18, 2018.
38. Pettersen VK, Antunes LCM, Dufour A and Arrieta MC: Inferring early-life host and microbiome functions by mass spectrometry-based metaproteomics and metabolomics. *Comput Struct Biotechnol J* 20: 274-286, 2022.



Copyright © 2023 Li et al. This work is licensed under a Creative Commons Attribution-NonCommercial-NoDerivatives 4.0 International (CC BY-NC-ND 4.0) License.